Research Square

Preprints are preliminary reports that have not undergone peer review.
They should not be considered conclusive, used to inform clinical practice,
or referenced by the media as validated information.

Integrated Multi-Port SIW Antenna with Self-Quadruplexing Capability and Circular Polarization Features for 6G Communication System

Ravi Bhushan Roy

rbhushan@jecjabalpur.ac.in

Jabalpur Engineering College

Prashant Kumar Jain

Jabalpur Engineering College

Prabhat Patel

Jabalpur Engineering College

Article

Keywords: MIMO Antenna, SIW, Circular Polarization

Posted Date: November 5th, 2026

DOI: https://doi.org/10.21203/rs.3.rs-11422238/v1

License: This work is licensed under a Creative Commons Attribution 4.0 International License.
Read Full License

Additional Declarations: No competing interests reported.

Integrated Multi-Port SIW Antenna with Self-Quadruplexing Capability and Circular Polarization Features for 6G Communication System

Ravi Bhushan Roy[1*], Prashant Kumar Jain[2], Prabhat Patel[3]
[1,2,3]Department of Electronics & Telecommunication Engineering, Jabalpur Engineering College, Jabalpur, 482 011, Madhya Pradesh, India
rbhushan@jecjabalpur.ac.in[*], pjain@jecjabalpur.ac.in, ppatel@jecjabalpur.ac.in

Abstract: A thin, small substrate integrated waveguide (SIW)-based antenna intended for quad-band operation is presented in this study. The design is straightforward and simple to use. The top surface of the SIW cavity is divided into four various radiating patches fed with a printed line. The antenna achieves peak gains of 5.12 dBi, 6.0 dBi, 5.8 dBi, and 5.55 dBi while operating 5.3 GHz, 5.7 GHz, 6.8 GHz, and 7.6 GHz. The antenna maintains isolation over 30 dB. Because of its design, each resonant frequency may be changed with a single parameter without influencing other aspects of performance. Additionally, circular polarization feature has been added to all four-operating band by loading stair shaped slot with each radiator. To confirm the findings, a prototype is built on FR-4 substrate and put through experimental testing. The antenna is ideal for 6G Communication system.

Keywords: MIMO Antenna, SIW, Circular Polarization

I. Introduction

Research on multi-band and multifunctional antenna designs has intensified due to the growing need for small and portable wireless devices. These antennas maintain structural simplicity and compactness while enabling simultaneous multi-frequency operation [1-3]. However, external multiplexing networks are often needed for independent transmission and reception over many bands, increasing the complexity and footprint of the system. In order to overcome this constraint, Rammos and Roederer suggested the idea of a self-duplexing antenna that could operate in two bands without the need for additional multiplexing electronics, which would reduce the size and complexity of the system [4]. In later works, this strategy has been further expanded. Additionally, because of its intrinsic benefits, such as excellent radiation efficiency, enhanced gain, reduced profile, and compatibility with planar manufacturing technologies, SIW cavity-backed antennas have garnered a lot of interest [5-7].

The self-duplexing idea has been expanded to SIW cavity-backed topologies, providing improved compactness and favourable radiation properties including strong inter-port isolation and lower back-lobe levels. Many self-multiplexing antenna layouts have now been described for dual-band and triple-band operations, respectively, including self-duplexing [8-10] and self-

triplexing designs [11-13]. However, it is harder to provide enough isolation between excitation ports as their number rises. Higher-order self-multiplexing antennas are in increasing demand due to the expanding needs of next-generation wireless systems. In this regard, self-quadruplexing antennas that have recently been described allow for simultaneous operation over four different frequency bands [14-16]. However, the creation of a small, completely planar-fed self-quadruplexing antenna with enhanced port isolation and a methodical design approach is still a research problem.

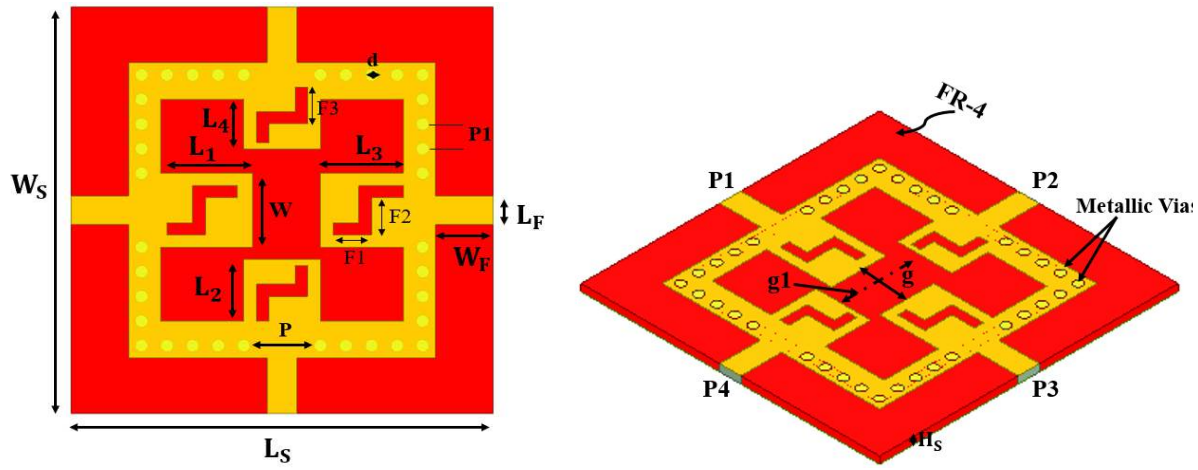
This paper presents a SIW-based self-quadruplexing antenna designed for quad-band operation with circular polarization features. The proposed antenna achieves a maximum gain of 6.0 dBi with a minimum inter-terminal isolation of 30 dB. Circular polarization features has been added with all four frequency band by loading stair slot. The remainder of the paper is structured as follows: Section II describes the antenna configuration, Section III details the design methodology and analysis, Section IV presents experimental validation, and Section V concludes the work.

II. Antenna Design Layout

Fig. 1 presents the upper view and 3D layout of designed radiator. In the proposed radiator, four-sided SIW cavity is fed with printed lines. This cavity is designed on FR-4 substrate having permittivity 4.4 and loss tangent 0.02. The cavity is surrounded with metallic vias, which shorts the patch with ground. To suppress leakage radiation, the via placement is optimized by ensuring that the via diameter and spacing satisfy the condition: $0.5p \leq d \leq 0.1\lambda_g$. This constraint ensures effective field confinement within the SIW structure, which helps in unidirectional radiation. The resonance of designed cavity can be calculated as follows [17]:

$$f_{mn0} = \frac{1}{2\pi\sqrt{\mu\varepsilon}}\sqrt{\left(\frac{m\pi}{L_1}\right)^2 + \left(\frac{n\pi}{W_1}\right)^2} \qquad (1)$$

where m & n= integer, μ = relative permeability, ε = relative permittivity of the substrate, L_1 & W_1 is effective length and width. The designed MIMO contains four patches of different length loaded with stair shaped slot for obtaining four bands with circular polarization features. Table-1 provides the optimum value of different parameters.



(a) (b)

Fig. 1 Layout of SIW built MIMO Radiator (a) Upper View (b) 3D View

Table-1 Optimum Size of various parameters of designed SIW MIMO

Symbol	Size (mm)	Symbol	Size (mm)
L_S	33.0	L_F	5.5
W_S	33.0	H_S	0.8
W_F	2.7	L_1	7.1
d	0.9	L_2	5.4
P	4.0	L_3	6.2
P1	2.0	L_4	4.6
W	5.8	F1	2.5
F2	4.8	F3	3.2
g	5.0	g1	4.7

III. Antenna Investigation

The electromagnetic solver ANSYS HFSS v18, which is based on the finite element technique (FEM), is used to model and simulate the suggested antenna. The next parts include experimental validation and detailed design analysis. A traditional rectangular SIW cavity is used to begin the antenna design, and its dimensions are determined using Equation (1). Two separate radiating elements with lengths L1 and L3 are then realized by perturbing the cavity. Fig. 2 shows the S-parameter variation independent excitation of each element via separate feed ports, P1 and P3. The optimal patch lengths are L1=7.1 mm and L3=6.2 mm based on thorough parametric research. Resonant frequencies at 5.3 GHz and 5.7 GHz are shown by the resultant antenna, which has a minimum isolation of 40 dB.

Fig. 3 shows the S-parameter variation independent excitation of each element via separate feed ports, P2 and P4. The optimal patch lengths are L2=5.4 mm and L4=4.6 mm based on thorough parametric research. Resonant frequencies at 6.58 GHz and 7.67 GHz are shown by the resultant antenna, which has a minimum isolation of 35 dB.

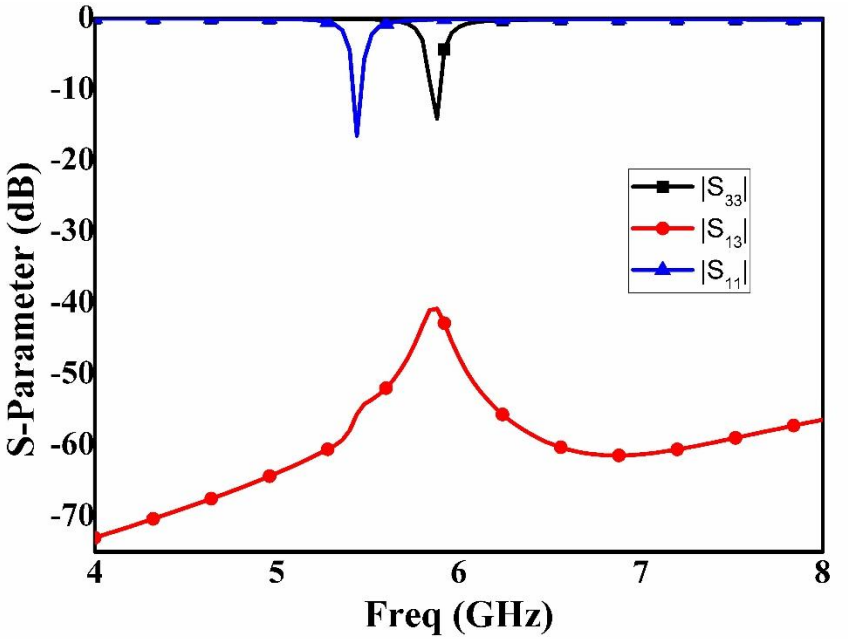


Fig. 2 Graph of S-parameter with radiating patch at port-1 and port-3

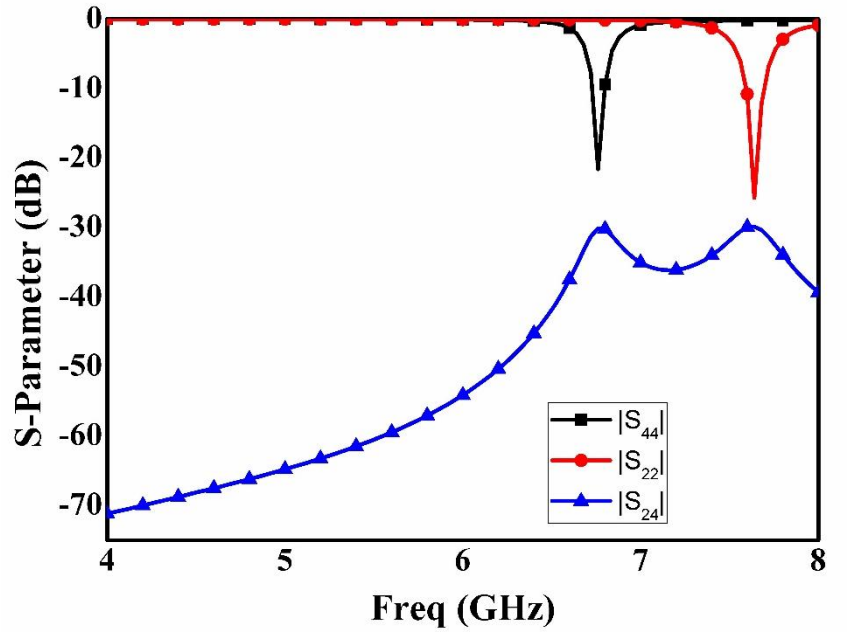


Fig. 3 Graph of S-parameter with radiating patch at port-2 and port-4

Fig. 4 presents S-parameter variation independent excitation of each element via separate feed ports, P1, P2, P3 and P4. It can be perceived from Fig. 4 that the four different resonances are obtained after integration of four different patches. The minimal inter-port isolation is found to decrease with the integration of four ports, reaching a value of around 30 dB between any two ports.

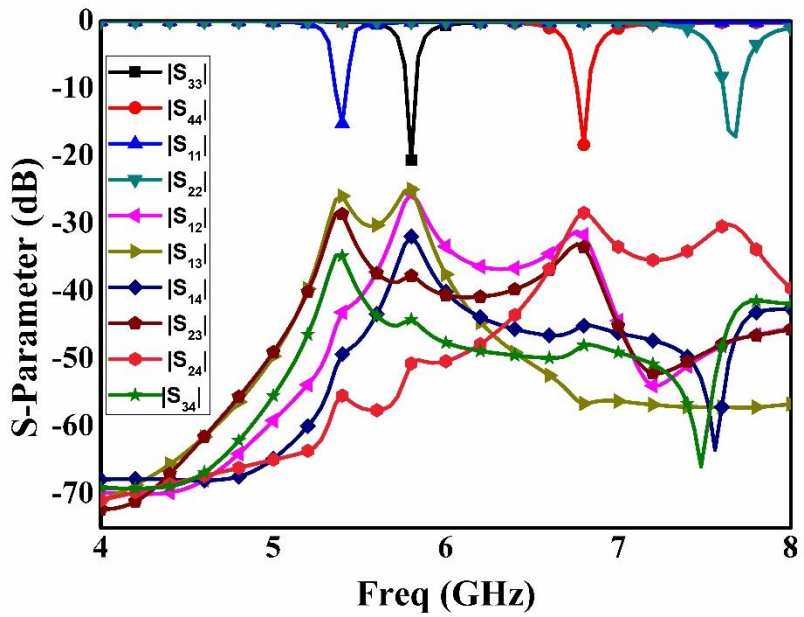


Fig. 4 Graph of S-parameter with all radiating patch at port-1, port-2, port-3 and port-4

Fig. 5 shows the electric field distributions of the suggested antenna under individual port excitations at various operating frequencies. It is clear that there is very little coupling to the other ports and that the field energy is mostly contained in the area around the stimulated port. The excellent inter-port isolation that the suggested design achieves is confirmed by this discovery.

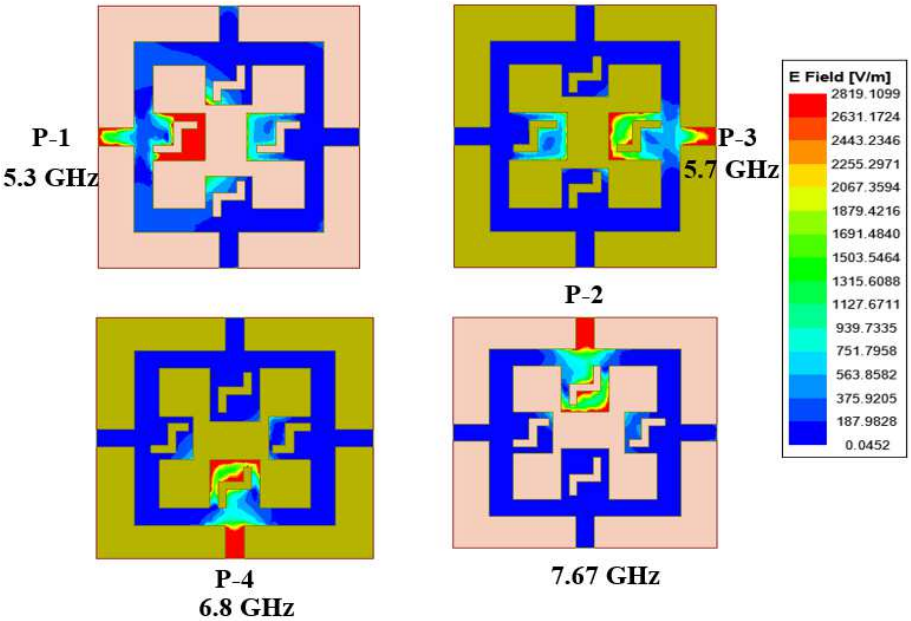


Fig. 5 Dispersion of E-field with multiple port stimulation at relevant resonance on top layer of suggested antenna

The variation of S-parameter with respect to L1 is depicted in Fig. 6. It is observed that the resonant frequency f_{S11} decreases with an increase in L1, whereas the other resonant

frequencies (f_{S22}, f_{S33}, and f_{S44}) remain largely unaffected, indicating independent tuning behaviour. The level of isolation of port-1 with other ports is more than 30 dB. In Fig. 6, the value of L1 ranges from 6.9-7.2 mm and corresponding frequency varies from 5.2-5.35 GHz.

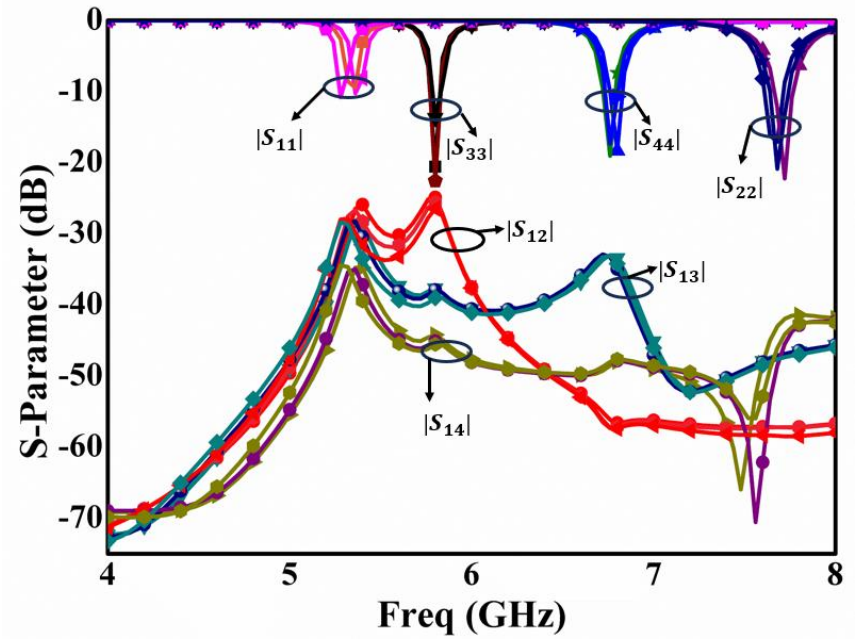


Fig. 6 Graph of S-parameter with change in value of L1

The variation of S-parameter with respect to L3 is depicted in Fig. 7. It is observed that the resonant frequency f_{S33} decreases with an increase in L3, whereas the other resonant frequencies remain largely unaffected. The level of isolation of port-3 with other ports is more than 25 dB. In Fig. 7, the value of L3 ranges from 6.0-6.4 mm and corresponding frequency varies from 5.6-6.2 GHz.

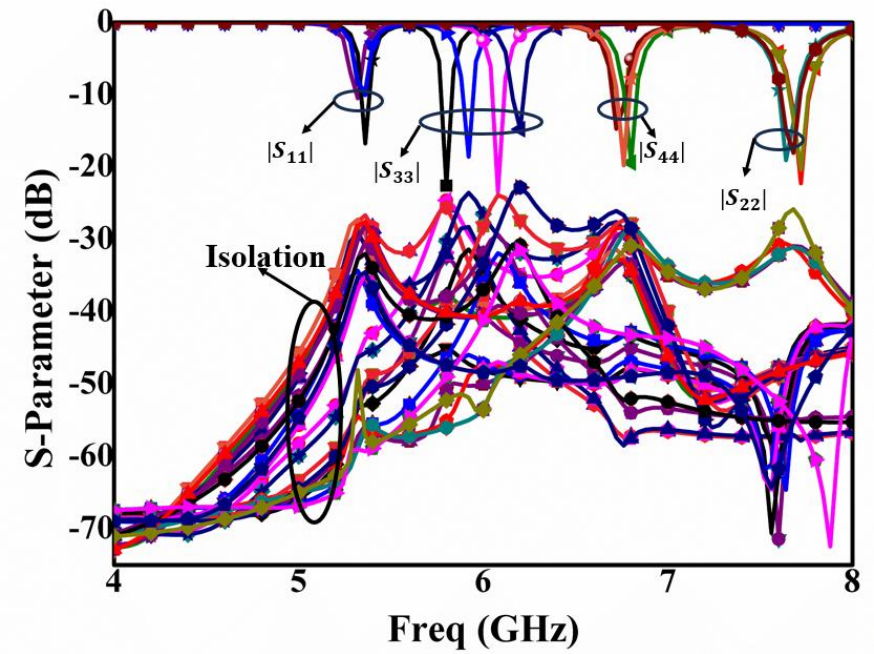


Fig. 7 Graph of S-parameter with change in value of L3

The variation of S-parameter with respect to L4 is depicted in Fig. 8. It is observed that the resonant frequency f_{S22} decreases with an increase in L4, whereas the other resonant frequencies remain largely unaffected. The level of isolation of port-2 with other ports is more than 35 dB. In Fig. 8, the value of L4 ranges from 4.5-4.7 mm and corresponding frequency varies from 7.55-7.9 GHz. Fig. 9 presents the S-parameter variation with change in L2. It can be perceived from Fig. 9 that resonance of port-4 changes with varying L2, while isolation of port-4 with other is more than 30 dB. The tuning range is in between 6.7-7.1 GHz for L2 varying from 5.3-5.5 mm.

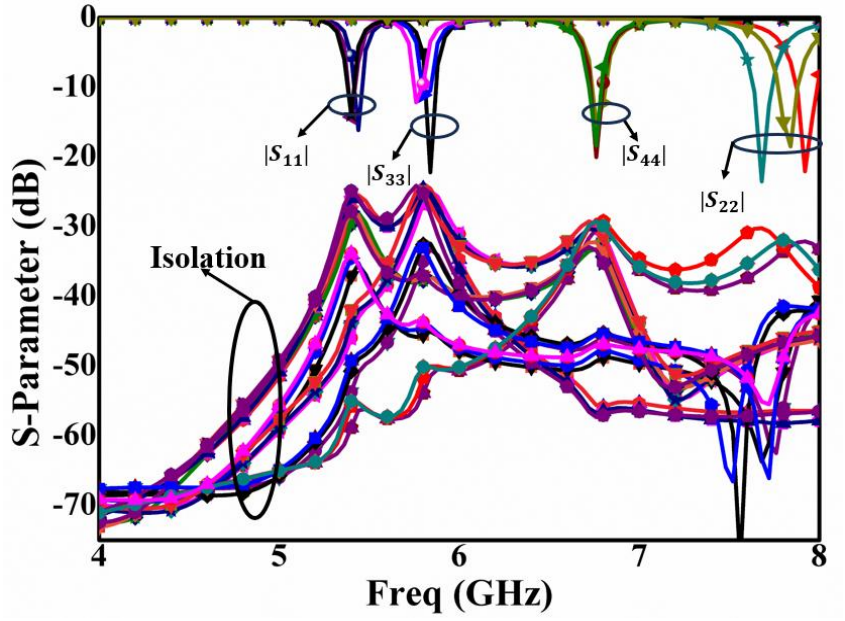


Fig. 8 Graph of S-parameter with change in value of L4

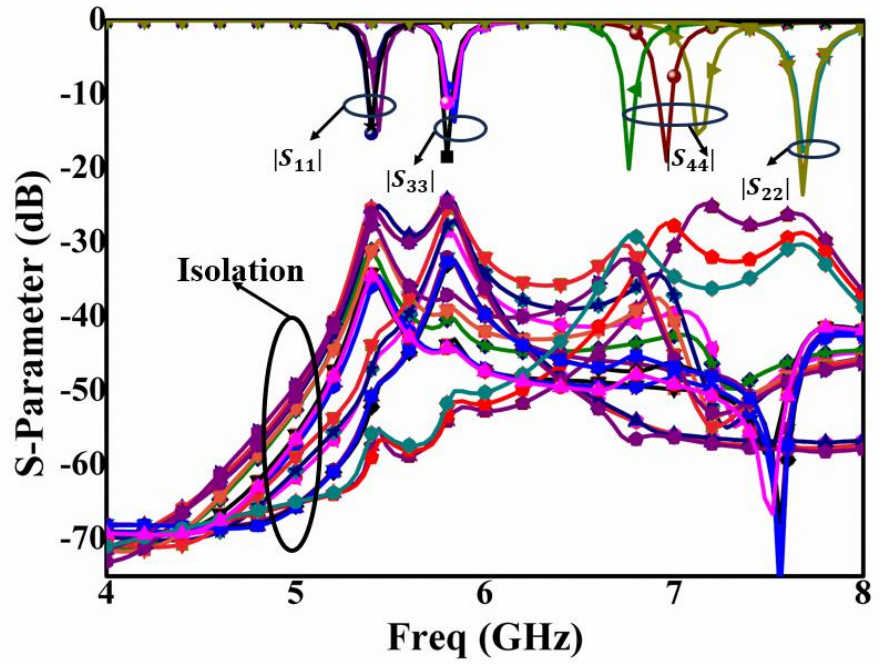


Fig. 9 Graph of S-parameter with change in value of L2

Fig. 10 shows the reflection coefficient graph with and without loading of stair formed slot in radiating patch. It can be seen from Fig. 10 that the loading of stair shaped slot lowers the resonance due to increment in the electrical length of radiating structure. Fig. 11 shows the axial ratio alteration with three different cases i.e. without loading slot, stair slot loading with same arm length and stair slot loading with unequal arm length. It can be seen from Fig. 11 that loading of stair slot having unequal arm length reduce the AR value to less than 3-dB in all frequency range. Stair shaped slot creates orthogonal degenerated mode, while unequal arm length produces 90^0 phase difference. This is the necessary condition for circular polarization features [18].

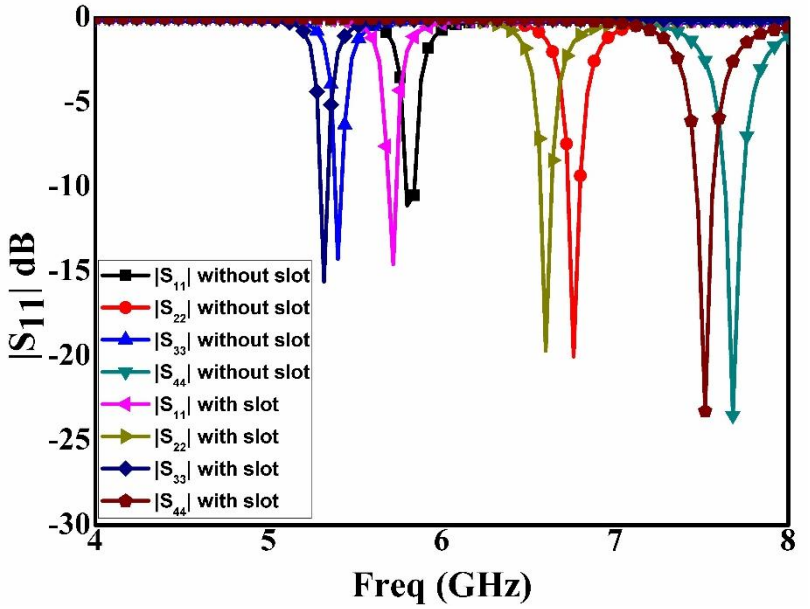


Fig. 10 Graph of reflection coefficient with and without slot loading

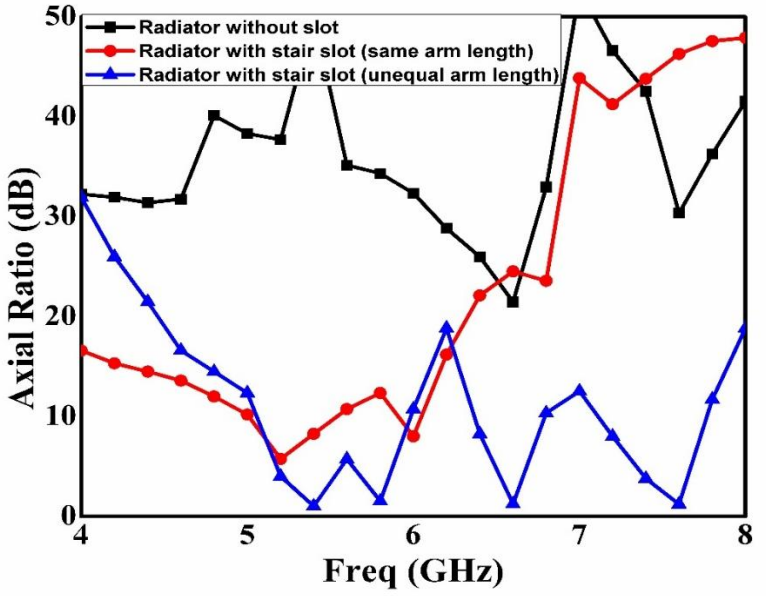
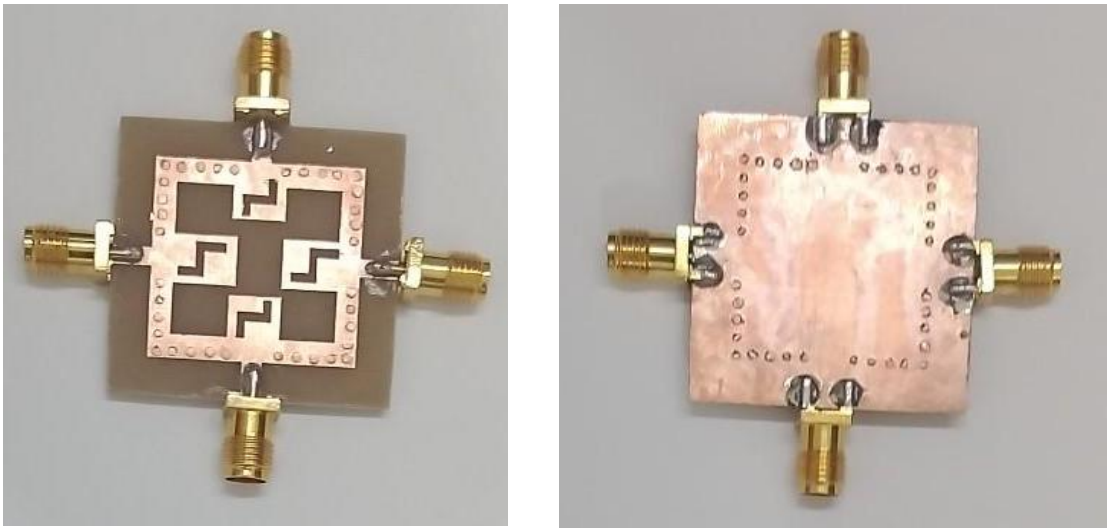


Fig. 11 Graph of AR with and without slot loading

IV. Experimental Outcomes

A Vector Network Analyzer (VNA), was used to experimentally analyse the manufactured prototype of the suggested antenna, as shown in Fig. 12. Because of its multi-port design, in order to assure precise S-parameter assessment, measurements are carried out by progressively stimulating each port while terminating the other ports with matching 50-Ω loads.



(a) (b)

Fig. 12 Photos of Antenna Prototype (a) Top View (b) Bottom View

Fig. 13 and Fig. 14 show the measured/simulated S-parameter responses for each port. Accurate impedance matching is confirmed by the reflection coefficients, which show excellent agreement with the simulated values. The inter-port isolation is still better than −35 dB for all port combinations, despite some variations in the measured isolation parameters.

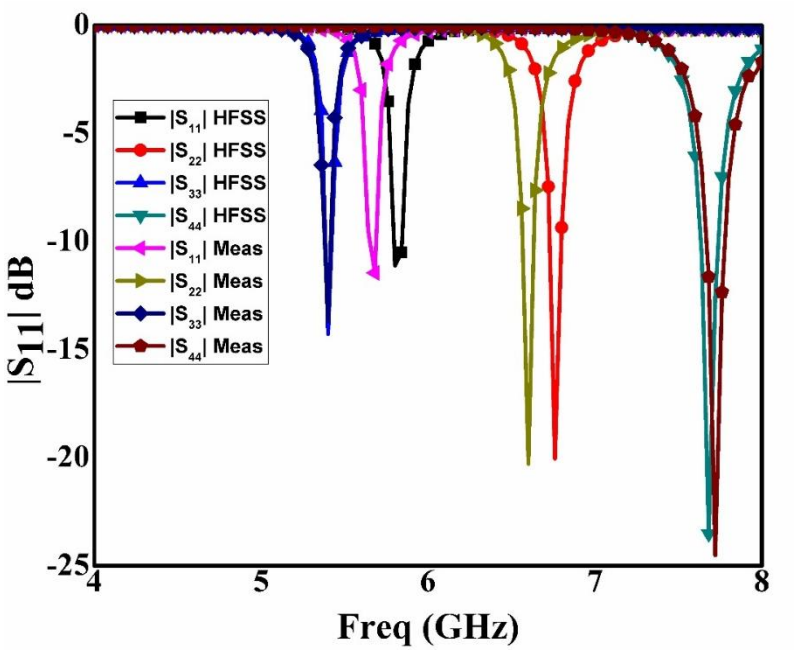


Fig. 13 Graph of Measured/simulated reflection coefficient with different ports

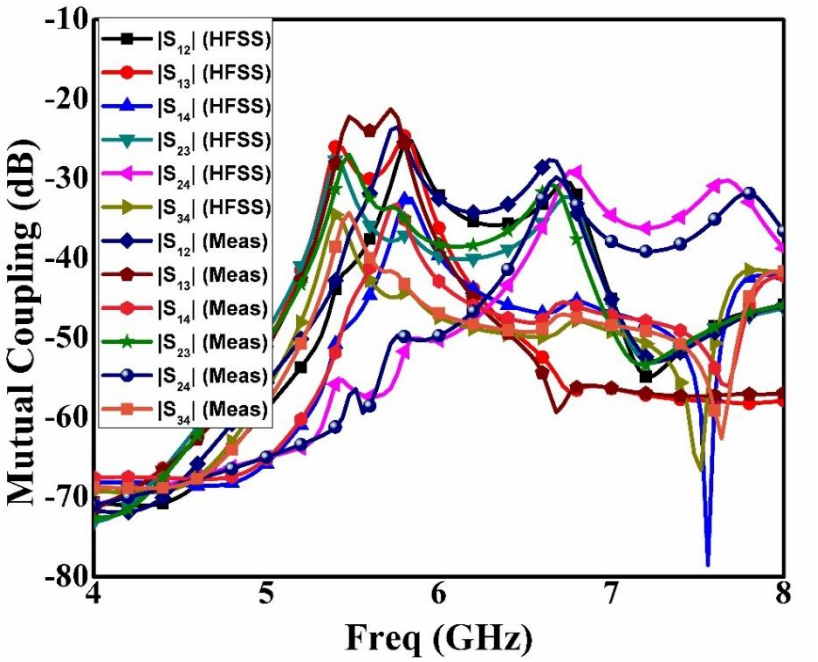


Fig. 14 Graph of Measured/simulated mutual coupling with different ports

Fig. 15 presents the measured/simulated axial ratio for designed radiator. It is measured using dual linear pattern technique [19]. There is good correlation between measured and simulated axial ratio. It can be confirmed from Fig. 15 that the proposed antenna supports CP waves within all frequency ranges.

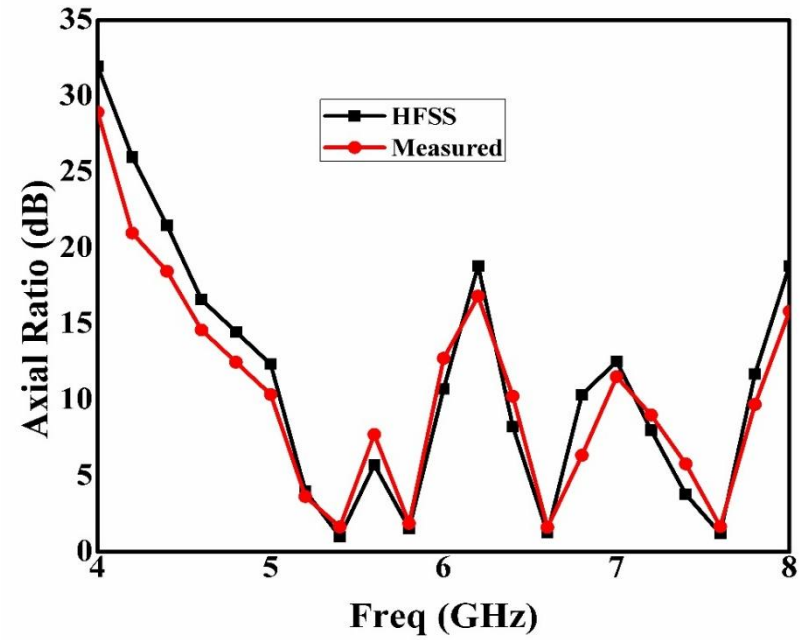


Fig. 15 Graph of Measured/simulated axial ratio

The LHCP/RHCP radiation patterns of antenna in XZ-plane are measured at all resonant frequencies and presented in Fig. 16. It is observed that the LHCP pattern is dominating over RHCP, which confirms the designed antenna acts as Left-handed circularly polarised. Fig. 17

presents the measured/simulated gain, which is measured in broadsided direction. It is measured using two antenna technique [19]. It can be seen from Fig. 17 that the gain value is in between 5.0-6.0 dBi within the working bands.

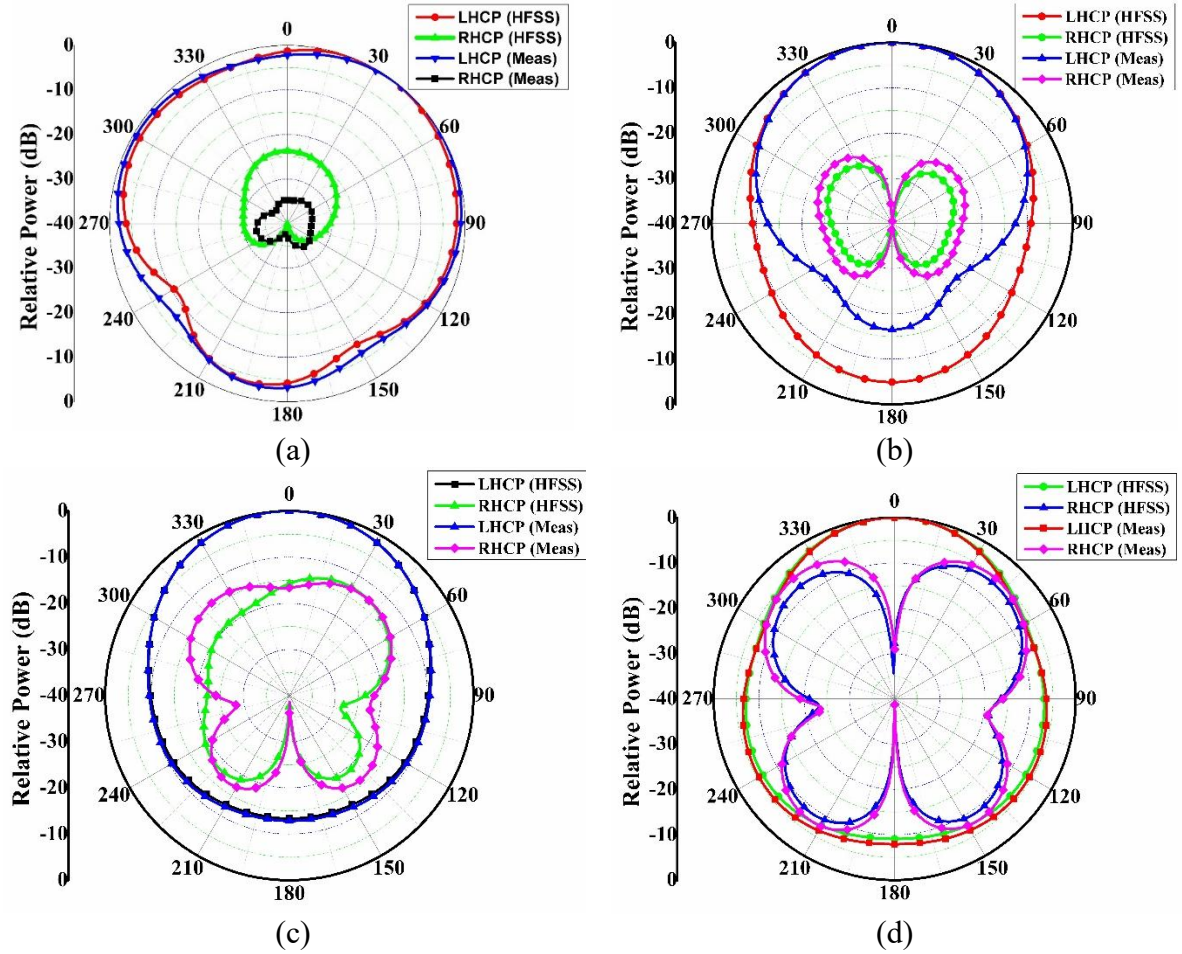


Fig. 16 Measured/Simulated LHCP/RHCP patterns in XZ plane (a) 5.3 GHz (b) 5.7 GHz (c) 6.8 GHz (d) 7.6 GHz

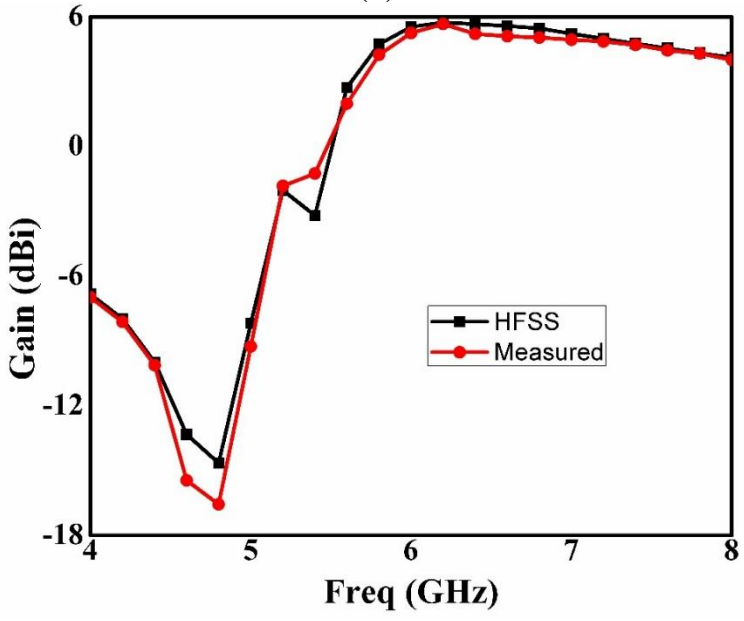


Fig. 17 Graph of Measured/simulated Gain

As shown in Table 2, the performance of the suggested four-port self-quadruplexing antenna is compared to previously published self-multiplexing configurations. Unlike traditional multiband antennas, self-multiplexing designs allow independent frequency adjustment and do away with the requirement for external multiplexing networks, which helps to reduce system size. The suggested antenna has better structural efficiency and compactness than current self-diplexing and self-triplexing designs. Furthermore, the suggested design exhibits better performance in terms of increased inter-port isolation, and improved gain as compared to documented self-quadruplexing antennas. Apart from this, the designed antenna supports circular polarization within the all four frequency bands.

Table-2 Performance Assessment of proposed circularly polarised SIW MIMO with existing ones

Ref.	Antenna Type	Bands	Frequencies	Max. Gain	Isolation	Circular Polarization
[8]	Self-diplexing	02	8.98, 11.22	4.3,4.2	≥25	No
[9]	Self-diplexing	02	8.55, 9.77	5.7, 5.9	≥18	No
[10]	Self-diplexing	02	9.5, 10.5	5.7, 5.9	≥25	No
[11]	Self-triplexing	03	7.8, 9.4, 9.8	4.2, 4.2, 4.0	≥22.5	No
[12]	Self-triplexing	03	5.57, 7.17, 7.65	4.10, 3.95, 3.54	≥21.3	No
[13]	Self-triplexing	03	4.14, 6.1, 8.32	4.26, 4.41, 5.27	≥20.8	No
[14]	Self-quadruplexing	04	4.8, 5.5, 6.6, 7.6	4.0-5.0	≥25	No
[15]	Self-quadruplexing	04	2.09–2.36	≈5.2	≥25	No
[16]	Self-quadruplexing	04	6.9–8.2	≈5.5	≥25	No
Proposed	Self-quadruplexing	04	5.3, 5.7, 6.8, 7.67	5.0-6.0	≥30	Yes

V. Conclusion

A small SIW-based four-port self-quadruplexing antenna with integrated circular polarization for quad-band C-band applications was reported in this study. The suggested design eliminates the need for external multiplexing circuits and permits independent frequency management by combining SIW cavity backing, self-quadruplexing capabilities, and circular polarization in a single planar structure. Across all bands, the antenna achieves gains of 5.0–6.0 dBi, inter-port isolation over 30 dB, and axial ratio below 3.0 dB. The design is validated by measured results, which accord well with models. The suggested antenna is appropriate for tiny C-band wireless

systems because it provides better compactness, increased isolation, and simultaneous circular polarization across all bands as compared to current designs.

Declarations

***Ethics approval and consent to participate:** Not Applicable

***Consent for publication:** I, Ravi Bhushan Roy, give my consent for the publication of identifiable details, which can include photograph(s) and/or videos and/or figures and/or details within the text ("Material") to be published in the above Journal and Article

*** Availability of data and materials:** Not Applicable

*** Funding:** No funds, grants, or other support was received.

*** Authors' contributions:** Conceptualization and Methodology [Ravi Bhushan Roy]; Writing - revised draft preparation: [Ravi Bhushan Roy]; Analysis and Investigation: [Prashant Kumar Jain]; Writing - original draft preparation and Supervision: [Prabhat Patel]

*** Disclosure of potential conflicts of interest:** There are no potential conflicts of interest.

*** Research involving Human Participants and/or Animals**: Not Applicable

*** Acknowledgements:** Not Applicable

***Data availability:** No datasets were generated or analysed during the current study

References

1. A. Mehdipour, A.R. Sebak, C.W. Trueman, T.A. Denidni, "Compact multiband planar antenna for 2.4/3.5/5.2/ 5.8-GHz wireless applications" IEEE Antennas Wireless Propag Lett. 2012; 11:144-147.2.
2. X. Sun, G. Zeng, H.C. Yang, "A compact quadband CPW-fed slot antenna for M-WiMAX/WLAN applications" IEEE Antennas Wireless Propag Lett. 2012; 11:395-398.3.
3. H. Liu, P. Wen, S. Zhu, "Quad-band CPW fed monopole antenna based on flexible pentangle-loop radiator. IEEE Antennas Wireless Propag Lett. 2015; 14:1373-1376.4.
4. E. Rammos, A. Roederw "Self-diplexing circularly polarized antenna" Proc IEEE/APS Symp Digest. 1990;803-806.5.
5. J. Lee, T. Koshio, N. Goto, "Self-diplexing antenna using the square patch with a hole" IEEE Microw Antennas Propag. 2002;149(1):7-10.6.
6. M. Nakano, H. Arai, W. Chujo, "Feed circuits of double-layered self-diplexing antenna for mobile satellite communications" IEEE Trans Antennas Propag. 1992;40(10):1269-1271.7.

7. H. Iwasaki, Y. Suzuki, “Dual frequency multilayered circular patch antenna with self-diplexing function” IET Electron Lett.1995;31(8):599-601
8. S. Mukherjee and A. Biswas, “Design of self-diplexing SIW cavity-backed slot antenna,” IEEE Antennas Wireless Propag. Lett., vol. 15, pp. 1775–1778, 2016.
9. S. Nandi and A. Mohan, “SIW-based cavity-backed self-diplexing antenna with plus-shaped slot,” *Microw. Opt. Technol. Lett.*, vol. 60, pp. 827–834, 2018.
10. A. A. Khan and M. K. Mandal, “Compact self-diplexing antenna using dual-mode SIW square cavity,” IEEE Antennas Wireless Propag. Lett., vol. 18, no. 2, pp. 343–347, 2019.
11. K. Kumar and S. Dwari, “SIW cavity-backed self-triplexing slot antenna,” IEEE Antennas Wireless Propag. Lett., vol. 16, pp. 3249–3252, 2017.
12. A. Kumar, D. Chaturvedi, and S. Raghavan, “Low-profile SIW cavity-backed self-triplexed slot antenna,” Int. J. RF Microw. Comput. Aided Eng., vol. 29, no. 3, 2019.
13. S. K. K. Dash, Q. S. Cheng, R. K. Barik; N. C. Pradhan; K. S. Subramanian “A compact triple-fed high-isolation SIW based self-triplexing antenna,” IEEE Antennas Wireless Propag. Lett., vol. 19, pp. 766–770, 2020
14. M. Naseri and M. Pourmohammadi, “SIW-based self-quadruplexing antenna for multi-band microwave applications,” IEEE Access, vol. 11, pp. 102345–102353, 2023
15. Y. Zhang, L. Wang, and X. Li, “A compact SIW slot-based quadruplexing antenna with high isolation,” Prog. Electromagn. Res. C, vol. 140, pp. 45–57, 2024
16. H. Liu, J. Chen, and Z. Wu, “Miniaturized CSRR-loaded SIW self-quadruplexing antenna with enhanced isolation,” Prog. Electromagn. Res. M, vol. 126, pp. 89–101, 2025.
17. S. Priya, S. Dwari, K. Kumar, M.K. Mandal, “Compact self-quadruplexing SIW cavity-backed slot antenna” IEEE Trans Antennas Propag. 2019;67(10):6656-6660.8
18. A. Sharma, G. Das, and R. K. Gangwar, “Dual polarized triple band hybrid MIMO cylindrical dielectric resonator antenna for LTE2500/WLAN/WiMAX applications” *Int J RF Microw. Comp. Aided Engg.,* vol. 26, pp. 763-772, 2016.
19. Stutzman W.L. and G.A. Thiele. 2013. “Antenna Theory and Design” *A John Wiley & Sons, New York, USA*